DALTON
FULL PAPER

Molecular structures of tetraborane(10) derivatives: *ab initio* calculations for $(CH_3)_2MB_3H_8$ (M = B, Al, Ga or In) and gas-phase electron diffraction studies of $(CH_3)_2AlB_3H_8$ and $(CH_3)_2GaB_3H_8$ †

Carole A. Morrison,[a] Bruce A. Smart,[a] Paul T. Brain,[a] David W. H. Rankin *,[a] and Anthony J. Downs[b]

[a] *Department of Chemistry, University of Edinburgh, West Mains Road, Edinburgh, UK EH9 3JJ*
[b] *Inorganic Chemistry Laboratory, University of Oxford, South Parks Road, Oxford, UK OX1 3QR*

Structural trends in the family of compounds $(CH_3)_2MB_3H_8$ (M = B, Al, Ga or In) have been investigated by *ab initio* molecular orbital calculations. In addition, the gas-phase molecular structures of $(CH_3)_2AlB_3H_8$ and $(CH_3)_2GaB_3H_8$ have been re-determined by gas-phase electron diffraction using the SARACEN method of structural analysis. Salient structural parameters (r_a^0) for the aluminium and gallium compounds were found respectively to be: *r*[B(1)···M(2)] 231.6(7), 234.2(8); *r*[B(1)–B(3)] 178.2(12), 178.9(23); *r*[B(1)–B(4)] 184.4(10), 184.3(23); *r*[B(1)–H(1,2)] 124.6(11), 121.6(18); *r*[M(2)–H(1,2)] 182.5(13), 186(6); *r*[B(1)–H(1,4)] 126.2(11), 122.9(18); *r*[B(4)–H(1,4)] 142.6(11), 140(3) pm; butterfly angle 123.8(20), 119.8(13)°.

The introduction of the SARACEN method [1,2] for the analysis of gas-phase electron diffraction (GED) data has led to a considerable improvement in the reliability and quality of structural refinements. In this method parameters which cannot be refined (both geometric and vibrational) are assigned restraints derived from an array of *ab initio* calculations. All geometric parameters and significant amplitudes of vibration are then refined as a matter of principle.

The series of compounds under investigation in this paper is based on the compound tetraborane(10) with one terminal BH_2 unit replaced by a $M(CH_3)_2$ unit (where M = B, Al, Ga or In). All four compounds have been investigated by *ab initio* calculations, and for $(CH_3)_2AlB_3H_8$ and $(CH_3)_2GaB_3H_8$ by electron diffraction. For these types of compound the structural information which can be obtained by electron diffraction alone is somewhat limited. The distances B–B, M–C and M–H_b are of similar length and therefore strongly correlated and, with the heavy atoms dominating the molecular scattering, locating the precise positions of the hydrogen atoms is a particularly difficult exercise. Consequently, in the original refinements reported for these compounds,[3] several parameters had to be fixed at assumed values and other assumptions had to be made to simplify the structural analysis. In addition, no reliable force fields were available to assess the effects of vibration. Thus, the preliminary structures reported for these molecules are of a very basic nature. With the availability of *ab initio* harmonic force fields and the development of the SARACEN method much improved structures can now be secured.

In addition to the new SARACEN refinements, the structural trends and similarities identified within the series $(CH_3)_2MB_3H_8$ by *ab initio* calculations are also discussed. Finally, the calculated structure of $(CH_3)_2InB_3H_8$ is compared with the experimental structure found in the solid phase.[4] This paper represents the final section of a structural exploration of tetraborane(10) derivatives, new molecular structures for the parent compound tetraborane(10)[2] and the derivative series $H_2MB_3H_8$ (where M = Al, Ga and In)[5] having been published previously.

† *Supplementary data available*: tables of *ab initio* geometries and energies and Cartesian coordinates from the 6-311G**/MP2 *ab initio* calculation for $(CH_3)_2MB_3H_8$ (M = B, Al, Ga or In), and final coordinates and least-squares correlation matrix for the SARACEN study of $(CH_3)_2MB_3H_8$ (M = Al or Ga). For direct electronic access see http://www.rsc.org/suppdata/dt/1998/2155/, otherwise available from BLDSC (No. SUP 57391, 14 pp.) or the RSC Library. See Instructions for Authors, 1998, Issue 1 (http://www.rsc.org/dalton).

Experimental

(a) *Ab initio* calculations

Theoretical methods. All calculations were carried out on a DEC Alpha APX 1000 workstation with the exception of the 6-31G*/MP2 and 6-311G**/MP2 $(CH_3)_2InB_3H_8$ calculations, which were carried out on the Rutherford Laboratory DEC Alpha 8400 5/300 workstation. The GAUSSIAN suite of programs was used throughout.[6]

Geometry optimisations. Details of the graded series of calculations performed for the dimethyl series of compounds are the same as for the hydride series reported in the preceding paper.[5] It is noted that, as no standard basis set for indium is available beyond the 3-21G* level, the basis set of Huzinaga[7] with an additional diffuse d-function (exponent 0.10), contracted to (21s, 17p, 11+1d)/[15s, 12p, 7+1d], was used for all higher level calculations. It is also worth repeating the special treatment used to describe the 3d and 4d electrons of gallium and indium, respectively. The default setting in the GAUSSIAN program placed these orbitals in the core region. A close examination of the calculated orbital energies, however, clearly showed these orbitals to lie closer in energy to the outer valence orbitals, rather than the inner core orbitals. Calculations were therefore performed with these orbitals defined as valence. Calculations beyond the MP2 level of theory were not attempted as higher level calculations were expected to give rise to only small changes in geometry, based on the evidence obtained from the larger series of calculations performed on the hydride analogues.[5]

Frequency calculations. Frequency calculations were performed at the 6-31G*/SCF level for $(CH_3)_2B_4H_8$, $(CH_3)_2AlB_3H_8$ and $(CH_3)_2GaB_3H_8$, confirming C_s symmetry as a local minimum in each case. Performing the 6-31G*/SCF frequency calculation in C_s symmetry for $(CH_3)_2InB_3H_8$ gave rise to one imaginary frequency (at -5 cm^{-1}), indicating that the C_s

Table 1 GED data analysis parameters for $(CH_3)_2AlB_3H_8$ and $(CH_3)_2GaB_3H_8$

Compound	Camera distance/mm	Weighting functions/nm^{-1}					Correlation parameter	Scale factor, k[a]	Electron wavelength[b]/pm
		Δs	s_{min}	sw_1	sw_2	s_{max}			
$(CH_3)_2AlB_3H_8$	128.16	4	72	92	280	328	0.1908	0.676(23)	5.8720
	285.06	2	24	42	130	160	0.2430	0.882(17)	5.1189
$(CH_3)_2GaB_3H_8$	128.45	4	68	100	230	288	0.0999	0.871(47)	5.1336
	285.06	2	24	44	130	166	0.2442	0.850(38)	5.0969

[a] Figures in parentheses are the estimated standard deviations. [b] Determined by reference to the scattering patterns of benzene vapour.

geometry is not a local minimum on the potential energy surface at this level. However, lowering the symmetry to C_1 resulted in the location of a local minimum less than 0.01 kJ mol^{-1} below the C_s geometry at the 6-31G*/SCF level, with the two methyl groups rotated by only 7°. It is not clear whether improvements in the theoretical treatment would lead to a C_s or a C_1 minimum for this compound; however, it is clear that the potential-energy surface is very flat and that any distortion from C_s symmetry is small. For $(CH_3)_2AlB_3H_8$ and $(CH_3)_2GaB_3H_8$ the force fields described by Cartesian force constants at the 6-31G*/SCF level were transformed into ones described by a set of symmetry coordinates using the program ASYM40.[8] Since no fully assigned vibrational spectra were available for these compounds, the force fields were adjusted using scaling factors of 0.94, 0.96 and 0.92 for bond stretches, angle bends and torsions, respectively.‡

(b) Gas-phase electron diffraction (GED)

GED data. The new refinements for $(CH_3)_2AlB_3H_8$ and $(CH_3)_2GaB_3H_8$ reported here are based on the original data sets[3] recorded on the Edinburgh apparatus. As with $H_2GaB_3H_8$ reported in the previous paper,[5] these compounds were found to react with the photographic emulsion of the GED plates, giving rise to data with higher than usual noise levels. Standard programs[9] were used for the data reduction with the scattering factors of Ross *et al.*[10] The weighting points used in setting up the off-diagonal weight matrices, the s ranges, scale factors, correlation parameters and electron wavelengths are given in Table 1.

GED model. As both $(CH_3)_2AlB_3H_8$ and $(CH_3)_2GaB_3H_8$ possess C_s symmetry, the same set of geometric parameters was used to describe the two structures. The model used was essentially based on that for $H_2GaB_3H_8$[5] with an additional two parameters [r(C–H) and angle H–C–M] to locate the positions of the hydrogen atoms in the two methyl groups attached to the M atom, which were assumed to possess local C_{3v} symmetry (see Fig. 1). Thus, twenty-two geometric parameters are required to define the structures fully in C_s symmetry, as given in Table 2. It should be noted that the new model system incorporates an additional five geometric parameters, compared with the model used in the original refinement.[3] These parameters allow a further five structural features to be investigated, namely the deviations of the bridging hydrogen atoms from the heavy-atom planes M(2)–B(1)–B(3) and B(1)–B(3)–B(4), the differences between the terminal B–$H_{endo/exo}$ and M–$C_{endo/exo}$ distances, and finally the tilting of the terminal BH_2 unit towards or away from the heavy-atom cage. Analogous parameters have been introduced in the recent re-refinements of B_4H_{10}[2] and $H_2GaB_3H_8$.[5]

The heavy cage atoms required four parameters to locate their positions: the weighted average and difference of the two B–B distances ($p_{1,2}$), r[B(1)···M(2)] (where M = Al or Ga) (p_3) and the butterfly angle (p_{20}) describing the angle between the planes B(1)–B(4)–B(3) and B(1)–M(2)–B(3). The remaining parameters locate the eight hydrogen atoms in the boron cage and the two methyl groups. Parameter p_4 is defined as r[M(2)–H(1,2)], p_5 as the weighted mean of all B–H distances in the molecule, and p_6 as the average B–H bridging distance minus the average B–H terminal distance. Parameter p_7 is the difference between the outer bridging distance B(4)–H(1,4) and the average of the two inner bridging distances B(1)–H(1,2) and B(1)–H(1,4); p_8 is r[B(1)–H(1,4)] minus r[B(1)–H(1,2)]; p_9 is the difference between rB(1)–H(1) and the average B–$H_{endo/exo}$ distance, and p_{10} rB–H_{endo} minus rB–H_{exo}. Parameters p_{11} and p_{12} are defined as the average of, and difference between, the two M–C distances, respectively, and p_{13} is the distance C–H. The six bond-angle parameters required are B(3)–B(1)–H(1) (p_{14}), C(2)$_{endo}$–M(2)–C(2)$_{exo}$ (p_{15}), H(4)$_{endo}$–B(4)–H(4)$_{exo}$ (p_{16}), the MC_2 and BH_2 tilt parameters (p_{17} and p_{18}), defined as the angles between the bisectors of the C(2)$_{endo}$–M(2)–C(2)$_{exo}$ and H(4)$_{endo}$–B(4)–H(4)$_{exo}$ wing angles and the planes B(1)–M(2)–B(3) and B(1)–B(4)–B(3), respectively, with positive values indicating tilting into the heavy atom cage, and finally the angle H–C–M (p_{19}). The last two parameters are the torsion angles, 'H(1,2) dip' and 'H(1,4) dip' (p_{21} and p_{22}), which define the elevation of the H(1,2) and H(1,4) bridging atoms above the B(1)–M(2)–B(3) and B(1)–B(4)–B(3) planes, respectively [*i.e.* the angles between the two sets of planes B(1)–M(2)–B(3) and B(1)–M(2)–H(1,2), and B(1)–B(4)–B(3) and B(4)–B(1)–H(1,4)].

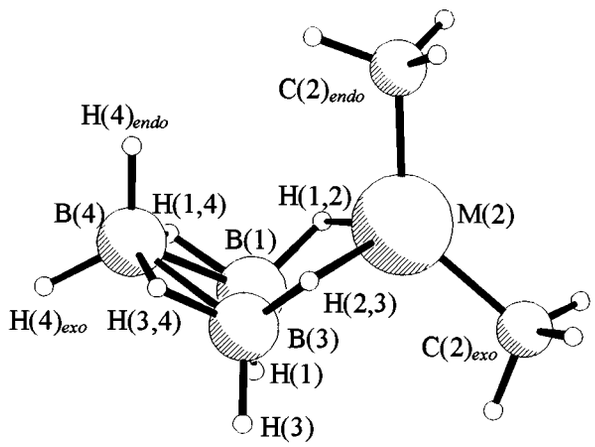

Fig. 1 Molecular framework of $(CH_3)_2MB_3H_8$ (M = B, Al, Ga or In)

Results and Discussion

(a) *Ab initio* calculations

In light of the many calculations performed on this series of compounds the full set of results obtained is confined to SUP 57391 Tables 1–4. Results obtained from the highest level calculations, 6-311G**/MP2, are reported for all four compounds in Table 3 of this paper.

A number of trends in geometry were observed to accompany improvements in basis set and level of theory, with the

‡ Scaling constants as used in the force fields for B_4H_{10}[2] and for $H_2GaB_3H_8$.[5]

Table 2 Geometric parameters (r_a^0/pm, angles in °) for the SARACEN refinements of $(CH_3)_2AlB_3H_8$ and $(CH_3)_2GaB_3H_8$

		Results[c]	
Parameters[a,b]		$Me_2AlB_3H_8$	$Me_2GaB_3H_8$
Independent			
p_1	av. r(B–B)	182.3(9)	182.5(22)
p_2	diff. r(B–B)	6.1(13)	5.3(13)
p_3	r[B(1)···M(2)]	231.6(7)	234.2(8)
p_4	r[M(2)–H(1,2)]	182.5(13)	186(6)
p_5	av. r(B–H)	126.5(7)	123.4(14)
p_6	av. r(B–H_b) − r(B–H_t)	11.6(12)	11.6(18)
p_7	diff. [r(B–H_b)] (outer − inner)	17.2(6)	17(3)
p_8	diff. [r(B–H_b)] (inner)	1.6(13)	1.3(13)
p_9	r[B(1)–H(1)] − av. r[B(4)–H_t]	−0.5(4)	−0.6(1)
p_{10}	diff. r(B–H_t) (*endo* − *exo*)	0.2(1)	0.3(3)
p_{11}	av. r[M–C]	193.9(5)	193.2(4)
p_{12}	diff. r(M–C) (*endo* − *exo*)	0.2(1)	0.3(3)
p_{13}	r(C–H)	107.2(4)	111.0(10)
p_{14}	B(3)–B(1)–H(1)	112.3(12)	111.6(13)
p_{15}	$C(2)_{endo}$–M(2)–$C(2)_{exo}$	132.0(23)	132.5(15)
p_{16}	$H(4)_{endo}$–B(4)–$H(4)_{exo}$	118.5(13)	118.5(13)
p_{17}	MC_2 tilt	−7.1(4)	−4.7(23)
p_{18}	BH_2 tilt	0.7(13)	0.5(21)
p_{19}	H–C–M	111.0(15)	108.6(10)
p_{20}	Butterfly angle	123.8(20)	119.8(13)
p_{21}	H(1,2) dip	13.4(13)	14.3(16)
p_{22}	H(1,4) dip	1.5(16)	−0.2(21)
Dependent			
	B(1)–B(4)–B(3)	57.8(4)	58.1(5)
	B(1)–M(2)–B(3)	45.3(3)	44.9(7)
	r[B(1)–B(3)]	178.2(12)	178.9(23)
	r[B(1)···B(4)]	184.4(10)	184.3(23)
	r[B(1)–H(1,4)]	126.2(11)	122.9(18)
	r[B(4)–H(1,4)]	142.6(11)	140(3)
	r[B(1)–H(1,2)]	124.6(11)	121.6(18)
	r[B(1)–H(1)]	119.4(10)	116.3(17)
	r[B(4)–$H(4)_{endo}$]	119.8(10)	116.8(17)
	r[B(4)–$H(4)_{exo}$]	119.6(10)	116.5(17)
	r[M(2)–$C(2)_{endo}$]	194.0(5)	193.4(4)
	r[M(2)–$C(2)_{exo}$]	193.8(5)	193.1(4)

[a] For definition of parameters see the text; b = bridging, t = terminal. [b] For atom numbering see Fig. 1. [c] For details of the refinements see the text. Estimated standard deviations (e.s.d.s) obtained in the least-squares refinement are given in parentheses.

most significant changes generally arising as a result of the introduction of electron correlation to the MP2 level. The main changes observed are summarised below.

Cage structure. The sensitivity of the cage distances to improvements in basis set and level of theory showed many parallels to the cage distance in the $H_2MB_3H_8$ series of derivatives reported in the previous paper.[5] In particular, r[B(1)–B(3)] in both sets of derivatives lengthened on average less than 1 pm on improving the basis set from 6-31G* to 6-311G** at both the SCF and MP2 level. The r[B(1)–B(4)] distance was found to be more sensitive to change; it increased by about 1–1.5 pm at both SCF and MP2 levels for the boron, aluminium and indium analogues, and shortened by just over 3 pm at SCF (remaining largely unaffected at the MP2 level) for the two gallium compounds. This difference in behaviour for the gallium compounds can largely be attributed to the poor quality of the 6-31G* basis set, which is deficient in the number of basis functions describing the core region of such a large atom.

The introduction of electron correlation had similar effects for all four compounds in both series, with r[B(1)–B(3)] shortening by about 2 pm with both the 6-31G* and 6-311G** basis sets. In contrast, r[B(1)–B(4)] was found to be less affected by electron correlation in the $(CH_3)_2MB_3H_8$ series than in the $H_2MB_3H_8$ series. It shortened by 1–2 pm in $(CH_3)_2B_4H_8$ for

Table 3 Structural trends observed in the $(CH_3)_2MB_3H_8$ series (M = B, Al, Ga or In) by *ab initio* (6-311G**/MP2) calculations (r_e/pm, angles in °)

		M			
Fragment	Parameter[a]	B	Al	Ga	In[b]
	Covalent radius[c]	88	125	125	140
	Ionic radius[c]	—	68	76	94
	Mulliken charge[c]	+0.2	+1.0	+0.7	+1.3
Cage	r[B(1)–B(3)]	173.5	178.2	178.6	179.7
	r[B(1)–B(4)]	185.3	184.5	184.1	183.5
	r[B(1)···M(2)]	189.9	230.4	232.6	256.3
	Butterfly angle	120.8	119.2	119.6	120.2
Bridge	r[B(1)–H(1,2)]	124.1	124.0	124.4	124.4
	r[M(2)–H(1,2)]	145.4	182.5	185.0	205.2
	r[B(1)–H(1,4)]	125.8	125.6	125.6	125.7
	r[B(4)–H(1,4)]	141.8	141.9	142.2	142.4
	B(1)–H(1,2)–M(2)	89.2	95.6	95.5	99.1
	H(1,4) dip	10.6	1.5	0.2	3.3
	H(1,2) dip	11.0	13.4	13.2	15.4
Terminal	r[M(2)–$C(2)_{endo}$]	160.3	195.3	195.6	217.2
	r[M(2)–$C(2)_{exo}$]	159.3	195.1	195.3	216.9
	r[B(4)–$H(4)_{endo}$]	119.4	119.4	119.5	119.6
	r[B(4)–$H(4)_{exo}$]	119.0	119.2	119.3	119.4
	r[B(1)–H(1)]	118.4	118.8	118.8	119.0
	$C(2)_{endo}$–M(2)–$C(2)_{exo}$	119.0	128.6	132.4	137.2
	$H(4)_{endo}$–B(4)–$H(4)_{exo}$	118.7	118.6	118.4	118.3
	B(3)–B(1)–H(1)	114.3	112.1	111.6	111.1

[a] For definition of parameters see the text. [b] For In basis set used see the text. [c] Ref. 11.

both basis sets (compared to 4–5 pm in B_4H_{10}), 4–5 pm in $(CH_3)_2AlB_3H_8$ (*cf.* 5–6 pm in $H_2AlB_3H_8$), *ca.* 3 pm in $(CH_3)_2GaB_3H_8$ (*cf.* 4–7 pm in $H_2GaB_3H_8$), and 2–3 pm in $(CH_3)_2InB_3H_8$ (3 pm in $H_2InB_3H_8$) for both basis sets.

The distance r(B···M) was found to vary in a similar fashion for the two series of derivatives on improving the basis set from 6-31G* to 6-311G**, resulting in a lengthening at the SCF and MP2 levels. The two exceptions were r(B···Al) and r(B···In) which shorten by 0.7 pm and 2.4 pm, respectively, at the SCF level. Electron correlation at the MP2 level resulted in a shortening of the r(B···M) distance in both series of derivatives. The effect was more pronounced in the $(CH_3)_2MB_3H_8$ series, with r(B···M) shortening by *ca.* 11 pm in $(CH_3)_2B_4H_8$ for both basis sets (*cf.* 4–5 pm in B_4H_{10}); 3–5 pm in $(CH_3)_2AlB_3H_8$ (*cf.* 2–4 pm in $H_2AlB_3H_8$); 7.5–10.5 pm in $(CH_3)_2GaB_3H_8$ (*cf.* 3–6.5 pm in $H_2GaB_3H_8$), and 9–11 pm in $(CH_3)_2InB_3H_8$ (7–9 pm in $H_2InB_3H_8$).

Bridge region. Of the three B–H bridging distances, r[B(4)–H(1,4)] was observed to be the most sensitive to changes in theoretical method, with many changes paralleling those found for the $H_2MB_3H_8$ series. In particular, improving the basis set from 6-31G* to 6-311G** resulted in a lengthening of all three B–H distances in the boron, aluminium and indium compounds in the two series by about 0.5 pm at both the SCF and MP2 levels. The analogous distances in the two gallium compounds behaved differently to the other members on the series, with r[B(1)–H(1,2)] increasing by about 1 pm, r[B(1)–H(1,4)] shortening by about 0.3 pm, and r[B(4)–H(1,4)] lengthening by about 3 pm at both the SCF and MP2 levels. Again, this difference in behaviour for the gallium compounds is principally a reflection of the poor quality of the 6-31G* basis set.

The introduction of electron correlation at the MP2 level showed several similarities in the two sets of derivatives with, for example, the inner bridging distances r[B(1)–H(1,4)] lengthening and r[B(1)–H(1,2)] shortening on average by 1 pm for all compounds. The most significant difference between the two sets of derivatives relate to the two boron compounds using both basis sets; the outer bridging distance r[B(4)–H(1,4)] shortens by almost 5 pm in $(CH_3)_2B_4H_8$ compared to just 1 pm

in B_4H_{10}. In contrast, the *r*[B(4)–H(1,4)] distance shortens by 1–2 pm in the aluminium and gallium compounds in both series of derivatives and by *ca.* 3 pm in the two indium compounds on improving the level of theory from SCF to MP2 using 6-31G* or 6-311G** basis sets.

The M–H bridging distance in the two derivative sets was also found to behave in a similar fashion, with *r*[Al(2)–H(1,2)] shortening by about 0.5 pm, *r*[Ga(2)–H(1,2)] shortening by an average of 5 pm, and *r*[In(2)–H(1,2)] shortening by about 1 pm on improvement of the basis set at both levels of theory. Electron correlation results in a change of less than 1 pm in *r*[M(2)–H(1,2)] (M = Al, Ga or In) irrespective of the basis set.

Terminal region. The B–H terminal distances in all eight compounds were found to be largely insensitive to change, with all distances varying on average by less than 0.5 pm with improvements in basis set and less than 1 pm for improvements in the level of theory. Similarly the M–C distances were found to vary by no more than 0.6 pm for basis set improvement and less than 1 pm (M = B or Al) or 2 pm (M = Ga or In) with electron correlation.

(b) Gas-phase electron diffraction (GED)

In the original refinements of $(CH_3)_2AlB_3H_8$ and $(CH_3)_2GaB_3H_8$ several structural assumptions had to be made since the amount of information that can be derived solely from the GED data is somewhat limited.[3] In particular, the B–B, M–C and M–H_b distances, being of similar length, are all subject to strong correlation, and locating the hydrogen atoms is a particularly difficult task as the heavy atoms dominate the molecular scattering. The following assumptions had to be made: (a) several parameters were fixed at values derived from the original B_4H_{10} study,[12] *i.e.* the two B–B distances, the angles B(3)–B(1)–H(1) and $H(4)_{endo}$–B(4)–$H(4)_{exo}$, the difference between the outer B(4)–H(1,4) and inner B(4)–H(1,4) bridging distances, and finally the difference between *r*[B(1)–H(1)] and the average $B(4)–H(4)_{endolexo}$ distance; (b) the difference between the two inner B–H_b distances was set at zero; (c) the bridging hydrogen atoms were taken to lie in the heavy-atom planes B(1)–M(2)–B(3) and B(1)–B(4)–B(3); and finally (d) as no force field was available, vibrational amplitudes were fixed at values in line with those determined for the related molecules B_4H_{10}[11] and $(CH_3)_2MBH_4$ (M = Al or Ga).[13]

In the earlier study[3] nine or ten of the seventeen geometric parameters used to describe the structures were successfully refined, along with three or four vibrational amplitudes. Final R_G values recorded were 0.159 for $(CH_3)_2AlB_3H_8$ and 0.139 for $(CH_3)_2GaB_3H_8$. The structures deduced were largely in accord with those of similar compounds. However, with almost half of the geometric parameters fixed at assumed values, several severe structural assumptions made and the adoption of a very crude approximation concerning vibrational effects, the quality of the original refinements was necessarily limited. As the SARACEN method allows the refinement of all geometric parameters and removes the need to make any structural assumptions in the GED model, a more flexible model can now be used, leading to much more reliable and realistic structures. In addition, the determination of reliable harmonic force fields by *ab initio* calculations removes the earlier assumptions concerning the effects of vibration on the molecular structures.

$(CH_3)_2AlB_3H_8$. The results obtained in the new refinement of the structure of $(CH_3)_2AlB_3H_8$ are given in Table 2. The radial-distribution curve [shown in Fig. 2(a)] is composed mainly of four peaks, with distances *r*[B(1)···Al(2)], *r*[Al(2)–$C(2)_{endolexo}$], *r*[B(1)–B(2)] and *r*[B(1)–B(3)] forming the dominant features. The parameters p_1 (the average B–B distance), p_3 [*r*B(1)···Al(2)], p_5 (the average B–H distance), p_{11} (the average Al–$C_{endolexo}$ distance) could all be refined freely, together with p_{13}

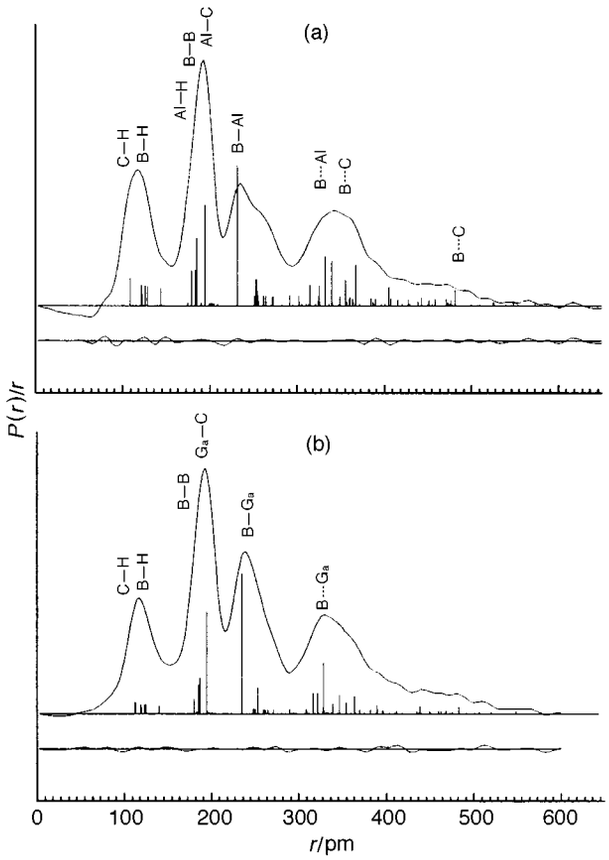

Fig. 2 Observed and final difference radial-distribution curves for (a) $(CH_3)_2AlB_3H_8$ and (b) $(CH_3)_2GaB_3H_8$. Before Fourier inversion the data were multiplied by $s\cdot\exp[(-0.000\ 02s^2)/(Z_M - f_M)(Z_B - f_B)]$ (M = Al or Ga)

[*r*(C–H)] and p_{19} (Al–C–H) which, with multiplicities of six, would be expected to be well defined by the GED data. In addition, the angles $C(2)_{endo}$–M(2)–$C(2)_{exo}$ (p_{15}), MC_2 tilt (p_{17}) and the butterfly angle (p_{20}) could also be refined to realistic values with reliable e.s.d.s. The remaining thirteen geometric parameters could be refined successfully only with the aid of flexible restraints (documented in Table 4) in accordance with the SARACEN method.§¶

Four amplitudes of vibration, corresponding to distances u_{13}[B(1)···Al(2)], u_{17}[B(1)···$C(2)_{endo}$], u_{18}[B(1)···$C(2)_{exo}$] and u_{21}[B(4)···Al(2)] could be refined. With the inclusion of twelve vibrational amplitude restraints (given in Table 5), a further seventeen vibrational amplitudes yielded to refinement (see Table 6). Thus, all the amplitudes associated with distances contributing greater than 10% weighting of the most intense

§ Each geometric restraint has a value and an uncertainty derived from the graded series of *ab initio* calculations. Absolute values are taken from the highest level calculation and uncertainties are estimated from values given by lower level calculations, or based on a working knowledge of the reliability of the calculations for electronically similar molecules.

¶ As a result of the large number of basis functions required to describe $(CH_3)_2AlB_3H_8$ and $(CH_3)_2GaB_3H_8$, it was not possible to perform calculations to a high enough level to display satisfactory convergence (see SUP 57391 Tables 2 and 3). However, the large array of calculations performed on the parent compound B_4H_{10} (see previous paper),[5] shows that the heavy cage atoms are much better described at the MP2 level of electron correlation than at the SCF level. Accordingly the uncertainty of 1 pm chosen for the cage parameter diff. *r*(B–B) (p_2) for both refinements is based on the variation revealed in the B–B cage distances of B_4H_{10} by calculations performed at the MP2 level and above. The derivation of the remaining geometric restraints is based on results obtained from the $(CH_3)_2AlB_3H_8$ and $(CH_3)_2GaB_3H_8$ series of calculations, and is documented in Table 4.

Table 4 Derivation of the geometric restraints used in the SARACEN refinements of $(CH_3)_2AlB_3H_8$ and $(CH_3)_2GaB_3H_8$ (*r*/pm, angles in °)

			Basis set/level of theory				
Compound		Parameter[a]	6-31G*/ SCF	6-311G**/ SCF	6-31G*/ MP2	6-311G**/ MP2	Value used
$(CH_3)_2AlB_3H_8$	p_2	diff. *r*(B–B)	8.7	9.0	6.0	6.3	6.3(10)
	p_4	*r*[Al(2)–H(1,2)]	182.1	181.9	183.2	182.5	182.5(10)
	p_6	av. B–H_b − av. B–H_t	11.9	12.4	10.7	11.4	11.4(10)
	p_7	diff. [*r*(B–H_b)] (outer − inner)	17.8	18.0	16.6	17.1	17.1(5)
	p_8	diff. [*r*(B–H_b)] (inner)	1.4	0.5	1.6	1.6	1.6(1)
	p_9	*r*[B(1)–H(1)] − av. *r*[B(4)–H_t]	−0.1	−0.2	−0.6	−0.5	−0.5(1)
	p_{10}	diff. *r*(B–H_t) (*endo* − *exo*)	0.2	0.2	0.2	0.2	0.2(1)
	p_{12}	diff. *r*(Al–C) (*endo* − *exo*)	0.2	0.3	0.3	0.2	0.2(1)
	p_{14}	B(3)–B(1)–H(1)	113.2	113.1	112.3	112.1	112.1(10)
	p_{16}	$H(4)_{endo}$–B(4)–$H(4)_{exo}$	119.3	119.5	117.7	118.6	118.6(10)
	p_{18}	BH_2 tilt	0.4	−0.3	0.0	0.8	0.8(10)
	p_{21}	H(1,2) dip	13.2	12.3	14.0	13.4	13.4(10)
	p_{22}	H(1,4) dip	0.5	0.1	0.2	1.5	1.5(13)
$(CH_3)_2GaB_3H_8$	p_2	diff. *r*(B–B)	10.6	7.0	6.1	5.5	5.5(10)
	p_4	*r*[Ga(2)–H(1,2)]	190.2	186.2	190.7	185.0	185.0(50)
	p_6	av. *r*(B–H_b) − av. *r*(B–H_t)	10.8	12.8	10.2	11.6	11.6(14)
	p_7	diff. [*r*(B–H_b)] (outer − inner)	14.8	19.2	14.7	17.2	17.2(20)
	p_8	diff. [*r*(B–H_b)] (inner)	1.6	−0.2	2.0	1.2	1.2(10)
	p_9	*r*[B(1)–H(1)] − av. *r*[B(4)–H_t]	−0.1	−0.2	−0.5	−0.6	−0.6(1)
	p_{10}	diff. *r*(B–H_t) (*endo* − *exo*)	0.0	0.2	0.1	0.3	0.3(2)
	p_{12}	diff. *r*(Ga–C) (*endo* − *exo*)	0.0	0.2	0.1	0.3	0.3(2)
	p_{13}	*r*(C–H)	108.6	108.6	109.4	109.4	109.4(15)
	p_{14}	B(3)–B(1)–H(1)	112.2	112.2	110.9	111.6	111.6(10)
	p_{15}	$C(2)_{endo}$–Ga(2)–$C(2)_{exo}$	129.9	131.2	131.2	132.4	132.4(12)
	p_{16}	$H(4)_{endo}$–B(4)–$H(4)_{exo}$	119.1	119.2	117.3	118.4	118.4(10)
	p_{18}	BH_2 tilt	2.2	−0.6	2.2	0.6	0.6(16)
	p_{21}	H(1,2) dip	12.8	12.0	14.0	13.2	13.2(12)
	p_{22}	H(1,4) dip	2.0	0.7	2.8	0.2	0.2(16)

[a] For definition of the parameters see the text. [b] For method of electron correlation used for Ga see the text.

Table 5 Derivation of vibration amplitude restraints for the SARACEN studies of $(CH_3)_2AlB_3H_8$ and $(CH_3)_2GaB_3H_8$

Compound	Parameter	Value[a]	Uncertainty[b]
$(CH_3)_2AlB_3H_8$	u_1[B(1)–B(3)]/u_{12}[B(1)–B(4)]	0.83	0.04
	u_2[B(1)–H(1)]	8.2	0.82
	u_3[B(1)–H(1,4)]	9.1	0.91
	u_4[B(1)–H(1,2)]	9.1	0.91
	u_5[B(4)–H(1,4)]	12.9	1.29
	u_8[Al–$C(2)_{endo}$]/u_9[Al–$C(2)_{exo}$]	1.0	0.05
	u_{10}[Al–H(1,2)]	12.6	1.26
	u_{14}[Al ··· $H(methyl)_{endo}$]/u_{15}[Al ··· $H(methyl)_{exo}$]	1.0	0.05
	u_{16}[$C(2)_{endo}$–$C(2)_{exo}$]	11.0	1.1
	u_{19}[Al–H(1,4)]/u_{20}[Al–H(1)]	0.96	0.05
	u_{22}[B(4) ··· $C(2)_{endo}$]	12.9	1.29
	u_{23}[B(4) ··· $C(2)_{exo}$]	21.8	2.2
$(CH_3)_2GaB_3H_8$	u_1[B(1)–B(3)]	6.8	0.68
	u_8[Ga(2)–$C(2)_{endo}$]/u_9[Ga(2)–$C(2)_{exo}$]	1.00	0.05
	u_{12}[B(1)–B(4)]	8.6	0.86
	u_{10}[Ga(2)–H(1,2)]	14.8	1.48
	u_{14}[Ga–$H(methyl)_{endo}$]/u_{15}[Ga–$H(methyl)_{exo}$]	1.0	0.05
	u_{16}[B(1)–$C(2)_{endo}$]/u_{17}[B(1)–$C(2)_{exo}$]	1.00	0.05
	u_{18}[Ga(2) ··· H(1,4)]	14.0	1.4
	u_{19}[Ga(2) ··· H(1)]	15.0	1.5

[a] Values for amplitude restraints calculated from 6-31G*/SCF force field. [b] Uncertainties are 5% of amplitude ratio, 10% of absolute values.

feature in the radial-distribution curve were determined. Values for the amplitude restraints were calculated directly from the scaled 6-31G*/SCF force field, with uncertainty ranges of 5% adopted for amplitude ratios or 10% for absolute values. Direct amplitude restraints were found to be necessary in the case of u_2[B(1)–H(1)], u_3[B(1)–H(1,4)] and u_4[B(1)–H(1,2)] as the normal practice of restraining ratios resulted in the return of unrealistic vibrational amplitude values in the least-squares refinement as a result of the high correlation effects.

Cage structure. The three cage distances *r*[B(1)–B(3)], *r*[B(1)–B(4)] and *r*[B(1) ··· Al(2)] refined to final values of 178.2(12), 184.4(10) and 231.6(7) pm, respectively, compared with their 6-311G**/MP2 *ab initio* values of 178.2, 184.5 and 230.4 pm. The butterfly angle (p_{20}) refined to 123.8(20)°, compared with its *ab initio* value of 119.2°.

Bridge region. The four bridging distances *r*[B(1)–H(1,4)], *r*[B(4)–H(1,4)], *r*[B(1)–H(1,2)] and *r*[Al(2)–H(1,2)] refined to 126.2(11), 142.6(11), 124.6(11) and 182.5(13) pm, respectively, in agreement with their 6-311G**/MP2 *ab initio* values to within one standard deviation.

Terminal region. The three terminal B–H distances, *r*[B(1)–H(1)], *r*[B(4)–$H(4)_{endo}$] and *r*[B(4)–$H(4)_{exo}$], refined to 119.4(10), 119.8(10) and 119.6(10) pm, respectively, in agreement with their respective 6-311G**/MP2 *ab initio* values to within one

Table 6 Selected bond distances (r_a/pm) and amplitudes of vibration (u/pm) obtained from the SARACEN refinement of $(CH_3)_2AlB_3H_8$

i	Atom pair	Distance	Amplitude[a,b]
1	B(1)–B(3)	178.7(12)	7.2(13)
2	B(1)–H(1)	121.8(10)	7.8(10)
3	B(1)–H(1,4)	128.2(11)	9.2(11)
4	B(1)–H(1,2)	126.1(12)	9.0(11)
5	B(4)–H(1,4)	143.9(11)	13.0(16)
6	B(4)–H(4)$_{endo}$	122.1(10)	8.3 fixed
7	B(4)–H(4)$_{exo}$	122.3(10)	8.3 fixed
8	Al(2)–C(2)$_{endo}$	194.8(5)	6.4(5)
9	Al(2)–C(2)$_{exo}$	194.5(5)	6.4(5)
10	Al(2)–H(1,2)	183.0(13)	12.7(16)
11	C–H(methyl)	108.7(4)	8.0(8)
12	B(1)–B(4)	185.2(10)	8.7(16)
13	B(1) · · · Al(2)	231.6(7)	9.9(5)
14	Al · · · H(methyl)$_{endo}$	253(7)	22(4)
15	Al · · · H(methyl)$_{exo}$	253(7)	22(4)
16	C(2)$_{endo}$ · · · C(2)$_{exo}$	355(3)	10.9(14)
17	B(1) · · · C(2)$_{endo}$	366.5(22)	9.3(21)
18	B(1) · · · C(2)$_{exo}$	340(3)	9(4)
19	Al(2) · · · H(1,4)	325(3)	6(6)
20	Al(2) · · · H(1)	314.6(13)	7(6)
21	B(4) · · · Al(2)	331(3)	19(9)
22	B(4) · · · C(2)$_{endo}$	405(3)	13.8(14)
23	B(4) · · · C(2)$_{exo}$	480.6(17)	20.5(24)

[a] Estimated standard deviations, obtained in the least-squares refinement, are given in parentheses. [b] Amplitudes which could not be refined are fixed at values derived from the 6-31G*/SCF scaled force field.

Table 7 Selected bond distances (r_a/pm) and amplitudes of vibration (u/pm) obtained from the SARACEN refinement of $(CH_3)_2GaB_3H_8$

i	Atom pair	Distance	Amplitude[a,b]
1	B(1)–B(3)	179.4(23)	6.7(9)
2	B(1)–H(1)	118.5(17)	8.3 fixed
3	B(1)–H(1,4)	124.5(18)	9.0 fixed
4	B(1)–H(1,2)	123.7(19)	9.2 fixed
5	B(4)–H(1,4)	140(3)	13.9 fixed
6	B(4)–H(4)$_{endo}$	119.4(17)	8.3 fixed
7	B(4)–H(4)$_{exo}$	118.7(17)	8.3 fixed
8	Ga–C(2)$_{endo}$	194.1(4)	5.9(7)
9	Ga–C(2)$_{exo}$	193.9(4)	5.8(7)
10	Ga–H(1,2)	186(6)	15.3(19)
11	C–H(methyl)	112.4(9)	7.6 fixed
12	B(1)–B(4)	185(23)	8.5(11)
13	B(1) · · · Ga	234.4(8)	7.5(9)
14	Ga · · · H(methyl)$_{endo}$	253(7)	11(3)
15	Ga · · · H(methyl)$_{exo}$	253(7)	11(3)
16	B(1) · · · C(2)$_{endo}$	364(5)	11(5)
17	B(1) · · · C(2)$_{exo}$	346(5)	12(6)
18	Ga · · · H(1,4)	321(3)	13.6(19)
19	Ga · · · H(1)	316.1(18)	14.6(20)
20	B(4) · · · Ga	328.0(15)	9.3(20)

[a] Estimated standard deviations, obtained in the least-squares refinement, are given in parentheses. [b] Amplitudes which could not be refined are fixed at values derived from the 6-31G*/SCF scaled force field.

standard deviation. The final two terminal distances, r[Al–C$_{endo}$] and r[Al–C$_{exo}$], at 194.0(5) and 193.8(5) pm, are slightly shorter than their predicted *ab initio* values of 195.3 and 195.1 pm. Of the six angles required to define the locations of the terminal atoms four parameters (p_{14}, p_{16}, p_{18} and p_{19}) all refined to values within one standard deviation of their *ab initio* values. Angle C(2)$_{endo}$–Al(2)–C(2)$_{exo}$ (p_{15}) refined to 132.0(23)°, within two e.s.d.s of its *ab initio* value of 128.6°, and the AlC_2 tilt angle (p_{17}) refined to −7.1(4)°, compared with its *ab initio* value of −4.6°, the negative value indicating a tilt out of the heavy atom cage.

$(CH_3)_2GaB_3H_8$. The results obtained for the new refinement of the structure of $(CH_3)_2GaB_3H_8$ are also given in Table 2. The radial-distribution curve [given in Fig. 2(b)] shows many similarities to that characterising $(CH_3)_2AlB_3H_8$ [see Fig. 2(a)] resulting from the similarities in molecular structure. The main difference between the two curves relates to the relative contributions from distances associated with gallium compared with aluminium. With an atomic number more than twice that of aluminium, gallium contributes much more to the molecular scattering through the atom pairs it forms, and contributions from other atom pairs necessarily give rise to less structural information. Consequently, only seven of the twenty-two geometric parameters in $(CH_3)_2GaB_3H_8$ could be refined freely {*viz.* p_1 av. r(B–B), p_3 r[B(1) · · · Ga(2)], p_5 av. r(B–H), p_{11} av. r(Ga–C$_{endo/exo}$), p_{17} GaC_2 tilt and p_{19} H–C–Ga}, compared with nine for $(CH_3)_2AlB_3H_8$. The derivation of the fifteen geometric restraints required to allow all the geometric parameters to refine is given in Table 4. Values adopted for the restraints were derived in the same way as for the aluminium analogue, with p_2 [diff. r(B–B)] based on the large array of calculations performed on the parent compound B_4H_{10}.[5]

In addition, three amplitudes of vibration, u_{13}[B(1) · · · Ga(2)], u_{15}[B(1) · · · C(2)$_{endo}$] and u_{16}[B(1) · · · C(2)$_{exo}$], could be refined freely. A further nine were successfully refined with the inclusion of eight amplitude restraints (given in Table 5), resulting in the refinement of all amplitudes associated with distances contributing greater than 10% weighting of the most intense feature in the radial-distribution curve (see Table 7).

Cage structure. The three cage distances r[B(1)–B(3)], r[B(1)–B(4)] and r[B(1) · · · Ga(2)] refined to 178.9(23), 184.3(23) and 234.2(8) pm, respectively, compared with their 6-311G**/MP2 *ab initio* values of 178.6, 184.1 and 232.6 pm. The small standard deviation for r[B(1) · · · Ga(2)] reflects the dominant electron scattering properties of the gallium and boron atoms. The butterfly angle (p_{20}) refined to 119.8(13)°, compared with its *ab initio* value of 119.6°.

Bridge region. The four bridging distances, r[B(1)–H(1,4)], r[B(4)–H(1,4)], r[B(1)–H(1,2)] and r[Ga(2)–H(1,2)], refined to 122.9(18), 140(3), 121.6(18) and 186(6) pm, respectively, in agreement with their 6-311G**/MP2 *ab initio* values to within one or two standard deviations. The distance Ga(2)–H(1,2), with a standard deviation of 6 pm, was found to be poorly defined by the GED data as a result of its closeness to the B–B distances. In the derivation of the restraint for this parameter [185(5) pm] it was necessary to stipulate a large uncertainty to allow for the significant variation that occurs in this bond length with improvements in basis set and level of theory (see Table 4). Although the restraint is very flexible, it enabled the Ga(2)–H(1,2) distance to be determined with much greater confidence than was possible using the GED data alone.

Terminal region. The terminal B–H distances, r[B(1)–H(1)], r[B(4)–H(4)$_{endo}$] and r[B(4)–H(4)$_{exo}$], refined to 116.3(17), 116.8(17) and 116.5(17) pm, in agreement with their respective 6-311G**/MP2 *ab initio* values to within two standard deviations. The distances Ga–C$_{endo}$ and Ga–C$_{exo}$ [like r(Al–C$_{endo}$) and r(Al–C$_{exo}$) in $(CH_3)_2AlB_3H_8$] refined to values slightly shorter than their predicted *ab initio* values [193.4(4) and 193.1(4) pm by GED, 195.6 and 195.3 pm *ab initio*]. Four of the six angles required to define the locations of the terminal atoms, p_{14-16} and p_{18}, refined to values within one standard deviation of their 6-311G**/MP2 *ab initio* values. Parameters p_{17}, MC_2 tilt, and p_{19}, H–C–Ga, refined freely to values of −4.7(23)° and 108.6(10)°, compared with their *ab initio* values of −4.8° and 110.6°.

The R_G factors recorded for these refinements were 0.081 [$(CH_3)_2AlB_3H_8$] and 0.111 [$(CH_3)_2GaB_3H_8$], the slightly high values being attributable to the rather high noise levels in the GED data resulting from fogging of the photographic plates by the $(CH_3)_2MB_3H_8$ vapours. With all twenty-two geometric parameters and all significant vibrational amplitudes refining, the structures are the best that can be obtained using all avail-

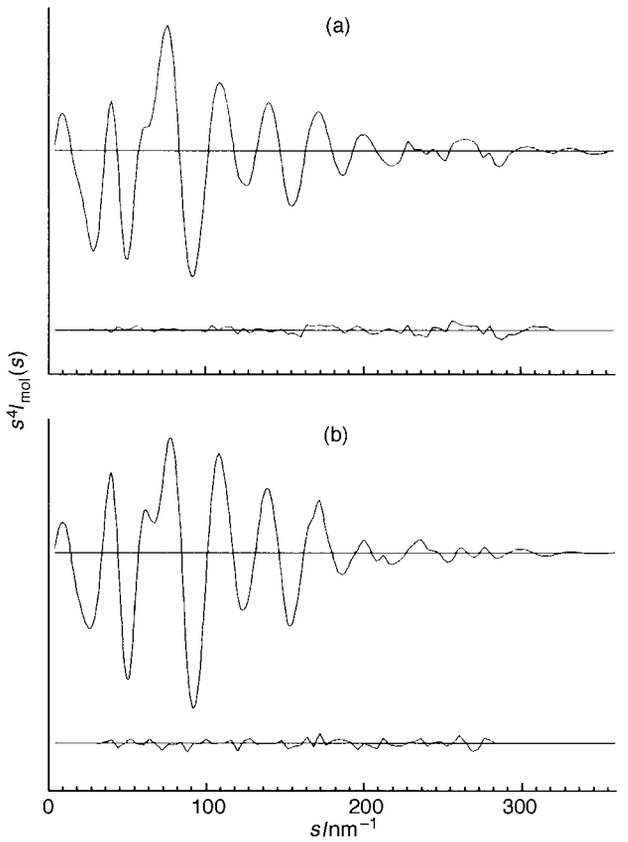

Fig. 3 Observed and final difference combined molecular scattering curves for (a) $(CH_3)_2AlB_3H_8$ and (b) $(CH_3)_2GaB_3H_8$. Theoretical data were used in the s ranges for which no experimental data are available

able data, both experimental and theoretical, and all standard deviations should be reliable estimates, free from systematic errors resulting from limitations of the model. A selection of bond distances (r_a) and vibrational amplitudes (u) for $(CH_3)_2AlB_3H_8$ and $(CH_3)_2GaB_3H_8$ are given in Tables 6 and 7, respectively. Cartesian coordinates and final least-squares covariance matrices can be found in SUP 57391. The final radial-distribution curves and combined molecular scattering curves are shown in Figs. 2 and 3, respectively.

(c) Structural trends within the series $(CH_3)_2MB_3H_8$ predicted *ab initio*: the effects of changing M

The main structural changes predicted by the 6-311G**/MP2 *ab initio* calculations for the series of dimethyltetraborane(10) derivatives $(CH_3)_2MB_3H_8$ (M = B, Al, Ga or In) are given in Table 3. Many of the trends observed with this series parallel those found in the hydride series reported earlier, and can be summarised as follows.

Changes in M–B/H distances. As with the hydride derivatives,[5] the increasing values of r[B(1)···M(2)], r[M(2)–H(1,2)], on moving from B to In can be attributed largely to the increase in atomic (or ionic) radius of the atom M (see Table 3). Thus, significant changes in these bond distances occur on replacing boron with aluminium and gallium with indium, but small changes are also observed on replacing aluminium with gallium. As noted with the hydride series, a secondary factor may be the decrease in Mulliken charge calculated *ab initio* for atom M (also given in Table 3). As the oxidation state approaches +1 the system can be thought of as approaching the formulation $[(CH_3)_2M]^+[B_3H_8]^-$. This dissociation will result in r[B(1)···M(2)] and r[M(2)–H(1,2)] increasing by an amount greater than the radius of atom M. Note: with the formal charge assignment on atom M in the dimethyl series being closer to +1, the two distances are 1–4 pm longer compared to the hydride series.

Angles correlated with atom M. The angle $C(2)_{endo}$–M(2)–$C(2)_{exo}$ was found to widen in a manner largely correlating with the increasing size and decrease in charge calculated for atom M. With the formal Mulliken charge assignment on atom M approaching +1 (see Table 3), the C_2M unit will tend towards a linear structure. It is interesting to note that as the charge assignment is much closer to +1 in the dimethyl series than in the hydride, the angle $C(2)_{endo}$–M(2)–$C(2)_{exo}$ is wider than $H(2)_{endo}$–M(2)–$H(2)_{exo}$ by 1–3°. The bridging angle B(1)–H(1,2)–M(2) varied in accordance with the increasing distance B(1)···M(2). This angle was found to be *ca.* 1° wider in the dimethyl than in the hydride series, which can be attributed to the longer B(1)···M(2) distance observed in the dimethyl series, as described above.

Changes in the B_3H_8 fragment. As with the hydride series, the distance B(1)–B(3) was found to be affected by the size of the atom M, with a significant lengthening observed when B is replaced with Al, and a further slight lengthening when In replaces Ga. The distance was found to be less than 1 pm longer in the dimethyl series. The angle B(3)–B(1)–H(1) narrowed slightly on moving from B to In, possibly due to a correlation with r[B(1)–B(3)]. As observed with the hydrides, r[B(1)–B(4)] shortened slightly across the dimethyl series, which can be attributed to a greater Mulliken charge disparity between atoms B(1) and B(4) as M = B ⟶ In, resulting in the distance shortening slightly due to a simple electrostatic force.

The same general trend was observed in both sets of derivatives for the positions of the bridging hydrogen atoms above the BBB/M plane [the H(1,2) and H(1,4) dip angles], with a greater elevation of the bridging atoms above the B(1)–M(2)–B(3) plane [H(1,2) dip] than above the B(1)–B(4)–B(3) plane [H(1,4) dip]. This observation was accounted for in the hydride series by the tilting of the wing units. In the dimethyl series the MC_2 unit tilts‖ out of the cage by 5° (*cf.* hydride MH_2 3°) and the BH_2 unit tilts into the cage by 1° (M = Al ⟶ In), in accordance with the hydride series. Thus H(1,2) dip would be expected to be more pronounced in the dimethyl derivatives, and H(1,4) would be expected to be about the same for both sets of compounds. This was indeed found to be the case, with H(1,2) raised *ca.* 13° above the B(1)–M(2)–B(3) plane in the aluminium and gallium compounds (*cf. ca.* 10.5° in $H_2AlB_3H_8$ and $H_2GaB_3H_8$), rising to 15° in $(CH_3)_2InB_3H_8$ (*cf.* 14° in $H_2InB_3H_8$). The variation in H(1,2) dip angles observed across the series can probably be attributed to the increase in size of atom M, with H(1,2) forced higher above the B(1)–M(2)–B(3) plane to relieve steric strain. The H(1,4) dip angle was found to be consistent in each series, with the only significant discrepancy of 10.6° in $(CH_3)_2B_4H_8$ *vs.* 8.4° in B_4H_{10} explained by a H_2B *exo* tilt of −4.4° in the former, compared with −2.4° in the latter, resulting in the higher elevation of the H(1,4) [and H(3,4)] atom in $(CH_3)_2B_4H_8$. Once again, the *ab initio* value obtained for the H(1,4) dip angle in $(CH_3)_2GaB_3H_8$, at just 0.2°, appears to be anomalous compared with the rest of the series. However, a close scrutiny of the complete range of *ab initio* calculations carried out (see SUP 57391 Table 3) indicates a significant variation in this parameter from 0.2 to 2.8° which can be attributed mainly to improvements in basis set. An uncertainty of about 3° in the 6-311G**/MP2 value of 0.2° would make this parameter more consistent with the results obtained for the other members of the series.

Distances and angles unchanged by atom M. The distances B(1)–H(1,4), B(4)–H(1,4) and B(1)–H(1,2) and angle $H(4)_{endo}$–B(4)–$H(4)_{exo}$ an the butterfly angle were largely unaffected by

‖ Wing tilts as described in GED model.

Table 8 Comparison of some geometrical parameters for $(CH_3)_2InB_3H_8$ (r/pm, angles in °)

Fragment	Parameter	*Ab initio*	X-Ray diffraction (averaged values)[a]
Cage	r[B(1)–B(3)]	179.7	178.4(8)
	r[B(1)–B(4)]	183.5	180.5(10)
	r[B(1)···In(2)]	256.3	274.4(11)
	Butterfly angle	120.2	124(2)
Bridge	r[B(1)–H(1,4)]	125.7	115(4)
	r[B(4)–H(1,4)]	142.4	140(7)
	r[B(1)–H(1,2)]	124.4	112(5)
	r[In(2)–H(1,2)]	205.2	224(11)
	H(1,2) dip	15.4	14(3)
	H(1,4) dip	3.3	3(1)
	H(1,2)–In(2)–H(2,3)	95.5	81(2)
Terminal	r[In(2)–C(2)$_{endo}$]	217.2	210.6(1)
	r[In(2)–C(2)$_{exo}$]	216.9	210.5(1)
	C(2)$_{endo}$–In(2)–C(2)$_{exo}$	137.2	158.0(1)

[a] See ref. 4. Two molecules, of C_1 symmetry were located in the asymmetric unit. Parameters are averaged to C_s symmetry for direct comparison with the *ab initio* structure, and uncertainties are quoted to 1 σ.

the identity of atom M. With reference to the corresponding hydrides, the butterfly angle for $(CH_3)_2MB_3H_8$ was found to be wider by *ca.* 4° when M = B, 3° when M = Al or Ga, and 1° when M = In. This widening can probably be attributed to reducing steric strain between the $(CH_3)_{endo}$ group and H(4)$_{endo}$. The effect is dominant in the earlier members of the series where the distance between the two groups is smaller, resulting in a larger opening of the cage to accommodate the $(CH_3)_{endo}$ group.

(d) $(CH_3)_2InB_3H_8$: comparison of *ab initio* and X-ray diffraction molecular structures

The final aspect of this work involved drawing a comparison between the molecular structure of $(CH_3)_2InB_3H_8$ deduced by *ab initio* calculations and the structure determined by X-ray diffraction (see Table 8).[4] *Ab initio* calculations determine the molecular structure of one discrete molecule which, in the absence of GED or any other experimental structural results for the gaseous molecule, represents the closest approach to the gas-phase structure that can be achieved at the present time. A direct comparison of the geometric parameters obtained *ab initio* with those determined by X-ray diffraction of a single crystal is therefore expected to identify differences between the gas- and solid-phase structures.

A word of caution should be entered, however, in making this type of comparison. Differences in molecular structure are to be expected as a consequence of the fundamental differences in the two techniques. Firstly, the definition of bond length is different: *ab initio* methods calculate the difference between the positions of atomic nuclei whilst X-ray diffraction measures the difference between centres of electron density. Secondly, the *ab initio* geometry is a static, vibration-free equilibrium structure; the crystal structure, measured at 150 K,[4] is subject to vibrational and librational averaging effects. For these reasons only fairly gross structural differences between the two sets of results have been considered significant.

The main structural differences, X-ray *vs. ab initio*, were found to centre around the indium atom, with (i) r[B(1)···In(2)] approximately 20 pm longer, (ii) the internal cage angle H(1,2)–In(2)–H(2,3) approximately 15° narrower, and (iii) C(2)$_{endo}$– In(2)–C(2)$_{exo}$ approximately 20° wider in the solid phase compared with the discrete structure calculated *ab initio*. The explanation for these structural differences is evident upon closer examination of the crystal structure: two neighbouring molecules interact with the indium centre through hydrogen H(1) atoms, effectively increasing the co-ordination number of the indium centre from four to six. As a result of this change in co-ordination H(1,2)–In(2)–H(2,3) will narrow, r[B(1)···In(2)] will lengthen to maintain the r[B(1)–B(3)] distance, and C(2)$_{endo}$–In(2)–C(2)$_{exo}$ will widen to force the two methyl groups apart and thereby accommodate the two new co-ordinating species.

In short, the changes reflect the greater ionic character of the compound in the crystal structure compared to that calculated, and the increased metallic character of the heavier Group 13 elements. Indium is characterised by adopting a high co-ordination number (typically six), and by forming solids with potential anionic partners manifesting increased ionic character.

Acknowledgements

We thank the EPSRC for the financial support of the Edinburgh Electron Diffraction Service (grant GR/K44411) and the Edinburgh *ab initio* facilities (grant GR/K04194). We also thank Drs. Simon Aldridge, John Dain and Simon Parsons for the parts they played in the experimental characterisation of the compounds $(CH_3)_2MB_3H_8$ (M = Al, Ga or In); and Dr. Lise Hedberg (Oregon State University) for providing us with a copy of the ASYM40 program. We are grateful to the Rutherford Laboratory for their generous allocation of time on the DEC Alpha 8400/300 workstation. Finally, we thank the University of Edinburgh for funding a research studentship for C. A. Morrison.

References

1 A. J. Blake, P. T. Brain, H. McNab, J. Miller, C. A. Morrison, S. Parsons, D. W. H. Rankin, H. E. Robertson and B. A. Smart, *J. Phys. Chem.*, 1996, **100**, 12 280.
2 P. T. Brain, C. A. Morrison, S. Parsons and D. W. H. Rankin, *J. Chem. Soc.*, *Dalton Trans.*, 1996, 4589.
3 C. J. Dain, A. J. Downs and D. W. H. Rankin, *J. Chem. Soc.*, *Dalton Trans.*, 1981, 2465.
4 S. Aldridge, A. J. Downs and S. Parsons, *Chem. Commun.*, 1996, 2055.
5 C. A. Morrison, B. A. Smart, P. T. Brain, C. R. Pulham, D. W. H. Rankin and A. J. Downs, preceding paper.
6 M. J. Frisch, G. W. Trucks, H. B. Schlegel, P. M. W. Gill, B. G. Johnson, M. A. Robb, J. R. Cheeseman, T. Keith, G. A. Petersson, J. A. Montogomery, K. Raghavachari, M. A. Al-Laham, V. G. Zakrzewski, J. V. Ortiz, J. B. Foresman, J. Cioslowski, B. B. Stefanov, A. Nanayakkara, M. Challacombe, C. Y. Peng, P. Y. Ayala, W. Chen, M. W. Wong, J. L. Andres, E. S. Replogle, R. Gomperts, R. L. Martin, D. J. Fox, J. S. Binkley, D. J. Defrees, J. Baker, J. P. Stewart, M. Head-Gordon, C. Gonzalez and J. A. Pople, GAUSSIAN 94, Revision C.2, Gaussian, Inc., Pittsburgh, PA, 1995.
7 S. Huzinaga and M. Klobukowski, *J. Mol. Struct.*, 1988, **167**, 1.
8 L. Hedberg and I. M. Mills, ASYM40 version 3.0, update of program ASYM20, *J. Mol. Spectrosc.*, 1993, **160**, 117.
9 A. S. F. Boyd, G. S. Laurenson and D. W. H. Rankin, *J. Mol. Struct.*, 1981, **71**, 113.
10 A. W. Ross, M. Fink and R. Hilderbrandt, *International Tables for Crystallography*, ed. A. J. C. Wilson, Kluwer, Dordrecht, Boston and London, 1992, vol. C, p. 245.
11 D. D. Ebbing, *General Chemistry*, ed. M. S. Wrighton, Houghton Mifflin, Boston, 1987, ch. 7.
12 C. J. Dain, A. J. Downs, G. S. Laurenson and D. W. H. Rankin, *J. Chem. Soc.*, *Dalton Trans.*, 1981, 472.
13 M. T. Barlow, A. J. Downs, P. D. P. Thomas and D. W. H. Rankin, *J. Chem. Soc.*, *Dalton Trans.*, 1979, 1793.

Received 24*th February* 1998; *Paper* 8/01554F